

Structural, electronic, and dynamical properties of amorphous gallium arsenide: A comparison between two topological models

Normand Mousseau* and Laurent J. Lewis†

*Département de physique and Groupe de recherche en physique et technologie des couches minces (GCM), Université de Montréal,
Montréal, Québec, Canada H3C 3J7*

(Received 6 February 1997)

We present a detailed study of the effect of local chemical ordering on the structural, electronic, and dynamical properties of amorphous gallium arsenide. Using the recently proposed “activation-relaxation technique” and empirical potentials, we have constructed two 216-atom tetrahedral continuous random networks with different topological properties, which were further relaxed using tight-binding molecular dynamics. The first network corresponds to the traditional amorphous Polk-type network randomly decorated with Ga and As atoms. The second is an amorphous structure with a minimum of wrong (homopolar) bonds, and therefore a minimum of odd-membered atomic rings, and thus corresponds to the Connell-Temkin model. By comparing the structural, electronic, and dynamical properties of these two models, we show that the Connell-Temkin network is energetically favored over Polk, but that most properties are little affected by the differences in topology. We conclude that most indirect experimental evidence for the presence (or absence) of wrong bonds is much weaker than previously believed and that only direct structural measurements, i.e., of such quantities as partial radial distribution functions, can provide quantitative information on these defects in *a*-GaAs. [S0163-1829(97)09439-3]

I. INTRODUCTION

After 25 years of effort, the structure of amorphous materials, and how it affects the electronic and vibrational properties, remains largely unresolved. Most experimental probes yield information that is averaged out over rather large length scales and therefore lack the sensitivity to discriminate between various possible structural models of the same material. Techniques such as extended x-ray-absorption fine structure (EXAFS), while they can provide structural information at the atomic level, are often too imprecise to yield definite and unambiguous structural parameters. One must therefore proceed iteratively between models and experimental data in order to acquire the desired structural information.

In the case of amorphous semiconductors, progress in the development of satisfactory structural models has been hindered by difficulties in constructing “continuous random networks” (CRN’s) with different topologies, i.e., appropriate to different materials. The idea of representing the structure of amorphous semiconductors by CRN’s was first proposed by Zachariasen;¹ in this picture, the material is assumed to consist of a “collage” of tetrahedra quite similar to those found in the corresponding crystal but randomly connected through their vertices. Based on these ideas, the mechanical CRN constructed by Polk was found to provide a very satisfactory description of the topology of elemental amorphous semiconductors.²

For compound materials, however, the situation is not as clear: The building-block tetrahedra, if they exist, can be formed in many different ways, depending on the chemical identities of the atoms, the arrangement of which is determined by the bonding characteristics of the material. For example, in the case of the III-V compound GaAs, chemical ordering should predominate because the material is partly

ionic, i.e., the number of bonds between like atoms (“wrong bonds”) should be minimal. Ideally, a tetrahedron should consist of a Ga atom surrounded by exactly four As atoms (or vice versa), as is the case in a perfect (zinc-blende) GaAs crystal. The actual structure of the disordered material, therefore, will be determined by a balance between the cost of elastically deforming the network while maintaining perfect chemical ordering and the cost of introducing wrong bonds. In view of this, *a*-GaAs appears to be an ideal candidate for the realization of the Connell-Temkin model³—a CRN similar to Polk’s but without odd-membered atomic rings. (A ring is defined as a closed path between an atom and itself through a series of bonds). Indeed, in an unconstrained CRN, there are inevitably both even- and odd-membered rings. Since odd-membered rings necessarily bring about wrong bonds, which cost Coulomb energy, it is expected that the number of them will be minimal in *a*-GaAs, and ideally none as in the Connell-Temkin model if the cost in elastic deformation energy associated with this constraint is not too large.

As noted above, detailed experimental information regarding the structure of compound materials is in general difficult to obtain; this is particularly so in the case of *a*-GaAs because of the close similarity between the constituent elements. (They are near neighbors in the Periodic Table; in fact, the similarity in size is another reason why the topology of *a*-GaAs should correspond closely to that of the single-component Connell-Temkin model.) Experimental evidence for the presence (or absence) of wrong bonds in this material is indeed essentially nonexistent, while the question does not arise in elemental amorphous semiconductors, such as *a*-Si. It is therefore important, in order to understand on a local scale the topology of amorphous semiconductors, to examine idealized representations of the two different types of networks, viz., Connell-Temkin and Polk, and compare

them with experiment. This is the object of the present paper.

In a recent paper, we have shown that it is quite possible to construct a binary-compound network that contains essentially no odd-membered rings (i.e., wrong bonds), corresponding to an infinite Connell-Temkin model;⁴ for GaAs, this model is found to be energetically preferred over the Polk model, where both even- and odd-membered rings are present. Likewise, for elemental and/or nonionic tetrahedral semiconductors, the Polk-type model is preferred for entropic reasons: elastic costs associated with the constraint on the absence of odd rings are negligible but the limitation on rings restricts significantly the number of possible configurations. In this way, we have been able to achieve a direct structural comparison of materials differing on the intermediate length scale—*a*-Si and *a*-GaAs.

In the present paper, we extend this study and examine in detail the structural, vibrational, and electronic properties of amorphous GaAs as described by the two types of CRN's mentioned above. This provides unique and much-needed information on the effects of topology on the properties of amorphous semiconductors. Indeed, upon comparing different networks constructed using the same energy scheme, it is possible to isolate, in measured properties, those effects arising from topology from those due to the interactions between atoms—evidently something that cannot be done experimentally.

II. METHODOLOGY

The time scale on which chemical ordering takes place when a binary compound is cooled down from the liquid phase depends strongly on the ionicity of the material. For example, molecular-dynamics (MD) simulations on a time scale of picoseconds are sufficient to ensure proper ordering of silica (SiO₂),⁵ which has a Phillips ionicity of 2.09.⁶ In contrast, corresponding simulations of *a*-GaAs, which is only slightly ionic (0.22), have not given clear indication of chemical ordering. Whether these results reflect the actual structure of GaAs or limitations of MD simulations needs to be addressed using a different approach for constructing structural models.

One possibility is to bypass the dynamics of formation and devise an appropriate static structure optimization scheme; by “appropriate” we mean that will lead to a physically realistic structural model. The route followed need not be physical, however: the philosophy we adopt here is one where “the end justifies the means.” This argument will become evident in the discussion that follows, but one closely related precedent can be invoked—the celebrated Wooten-Winer-Weaire (WWW) algorithm for constructing models of *a*-Si (Ref. 7): In this approach, crystalline Si is amorphized through a sequence of bond-switching moves that are totally unphysical; yet, the final (converged) structure possesses much of the properties of real *a*-Si. The method cannot be employed in the case of compound semiconductors because it is the essence of it to introduce odd-membered rings and wrong bonds. (It involves breaking nearest-neighbor bonds and forming second-neighbor—thus wrong—bonds.) These limitations of the WWW algorithm, and/or absence of alternative models, have significantly hin-

dered the study of amorphous semiconductors over the last ten or so years.

The activation-relaxation technique (ART) recently proposed by Barkema and Mousseau⁸ provides a way to circumvent the restrictions of the WWW model.⁹ Given a model of interatomic potentials, which can be of any form—from purely empirical to fully *ab initio*, the method (which is event-based) forces relaxation through a series of *physical* moves in a configurational space reduced to a set of isolated energy minima connected together by paths going through saddle points on the configurational energy landscape. Since the moves are defined in the $3N$ -dimensional configurational space, where N is the number of atoms, the algorithm is completely independent of the structure in the three-dimensional real space. A move, therefore, can involve any number of atoms, and, in particular, be local or span the whole system; it is not limited to a predetermined list of events, such as bond switches in the manner of WWW or atomic exchanges. Further, since the configurational space is reduced to an (infinite) number of discrete points, events can be defined uniquely.

Full details and illustrations of the ART method can be found in Ref. 8; here we give a brief overview. An ART simulation starts with the system in a local minimum of the potential-energy surface. The configuration is then placed slightly out of equilibrium by operating a small change on the system, e.g., moving an atom in a random direction by a very small amount. The component of the force *parallel* to the displacement of the configuration is then inverted and the whole configuration pushed away from the nearby minimum following the *modified force*:

$$\vec{G} = \vec{F} - (1 + \alpha)(\vec{F} \cdot \Delta\hat{X})\Delta\hat{X}, \quad (1)$$

where \vec{G} and \vec{F} are both $3N$ -dimensional vectors, α is a dimensionless parameter (here set to 0.15) and \hat{X} is the unit-vector displacement from the local minimum to the current position. Equation (1) is iterated until the modified force (and thus also the real force) vanishes, indicating that a saddle point has been reached. The configuration is then pushed slightly away from the saddle point and relaxed to a new local minimum. This procedure is iterated until convergence, i.e., until no further changes in the total energy are observed.

A few remarks are in order: (i) Since the algorithm is defined in configurational space, there is no limit to the number of atoms that can be involved in a single event; for the materials studied here, events involving one to a few tens of atoms have been observed. (ii) In order to prevent the configuration from moving to close-by saddle points that are not significant at finite temperature, a repulsive force is introduced that excludes a region of width $\sim x_c$ around any local minimum:

$$F_{\text{rep}} = A(x - x_c); \quad (2)$$

here x is the scalar displacement of the configuration from the local minimum, x_c is a cutoff parameter, and A is the strength of the repulsive part. Both x_c and A are drawn, for each new event, from a linear random distribution: $0.3 < x_c < 1.3 \text{ \AA}$ and $0.5 < A < 1.5 \text{ eV/\AA}^2$. (iii) After each event, the volume of the system is optimized such as to mini-

mize the configurational energy. (iv) Both activation to the saddle point and relaxation to the nearest local minimum are performed using the Levenberg-Marquardt algorithm;¹⁰ this algorithm, which includes both the steepest-descent and the Hessian approaches, is fairly efficient around a minimum and does not misbehave far from it. (v) The optimization is performed using a multiple-configuration simulated-annealing approach; thus, each new event is accepted with a probability

$$P_{\text{accept}}(\{x_{i+1}\}) = \exp\left[-\frac{E(\{x_{i+1}\}) - E(\{x_i\})}{k_B T}\right], \quad (3)$$

where here the temperature is a nonphysical parameter. In practice, two configurations are run in parallel at different temperatures. After each step, the energies are compared and the configurations are switched according to a Metropolis rule. The use of multiple configurations allows for more efficient sampling of configurational space, permitting configurations to escape from dead-end minima, i.e., those that cannot lead directly to a lower-energy state.

The force \vec{F} in Eq. (1) is derived from an interatomic potential which, as noted above, can in principle be of any form. Evidently, the final, optimized structure will depend on the choice of potential. With respect to GaAs, there exists (to our knowledge) no satisfactory empirical potential for the disordered phase. Our own attempts in this regard using a recently proposed Tersoff-type potential¹¹ have led to structures in deep disagreement with experiments. For the present work, construction of the computer models proceeded in two stages under two sets of potentials: first, ART optimizations using modified Stillinger-Weber potentials (see below) were carried out; and second, the models were further relaxed under semiempirical tight-binding (TB) potentials. The reason for this “double-relaxation” approach is that while ART relaxations can in principle be done with the TB potentials, this remains a complicated and computer-intensive enterprise. Carrying out a “first pass” with empirical potentials allows optimized structures to be obtained rapidly, while the final TB relaxation provides a physically meaningful basis for the models; indeed, we have found the properties of our networks to be only little affected by the final TB relaxation, thus indicating the convergence and validity of the procedure.

III. MODEL PREPARATION

As discussed in the Introduction, we consider here two networks with different topologies; following Ref. 4, these are poetically labeled CRN-A and CRN-B. CRN-A corresponds to a Polk-type network, while CRN-B is Connell-Temkin like. Full details of the procedure used to prepare the models can be found in Ref. 4. In brief, both models, which contain 216 atoms each, were optimized first with ART under Stillinger-Weber potentials,^{12,8} then relaxed at zero temperature with *both* the Goodwin-Skinner-Pettifor (GSP) TB potential for Si (Ref. 13) *and* the Molteni-Colombo-Miglio (MCM) TB potential for GaAs.¹⁴ Thus we have in total four different 0-K, TB-relaxed models: CRN-A-Si, CRN-A-GaAs, CRN-B-Si, and CRN-B-GaAs, i.e., for each material, two models with different topologies. In the case of CRN-A-GaAs, a “label-switching” procedure was used to minimize

the number of wrong bonds; the resulting value, 14%, is as close as one can possibly get, for a finite-size system, to the theoretical value of 12% for optimal ordering on a Polk-type CRN.¹⁵

As discussed in Ref. 4, it is clear, after static TB relaxation, that CRN-A is entropically favoured over CRN-B for elemental amorphous semiconductors. In contrast, it is decidedly more advantageous for the compound material GaAs to adopt the CRN-B structure: the energy gain resulting from the elimination of wrong bonds is a sizeable 0.11 eV/atom. A detailed comparison between Si and GaAs is given in Ref. 4; we only discuss, here, the two models for GaAs, viz., CRN-A-GaAs and CRN-B-GaAs, hereafter referred to simply as CRN-A and CRN-B.

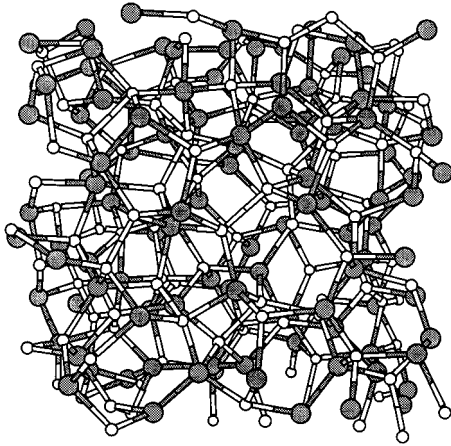
Following the static TB simulations referred to above, models CRN-A and CRN-B were further relaxed at 300 K using MD for a total of 7.0 ps. Although this is a fairly short period of time, it is enough to ensure that both models have evolved into deep local minima of the potential-energy surface. In order to verify this, we have also annealed the samples at 700 K during 8.8 ps before running again at 300 K for 3.5 ps and 10 K for 0.9 ps. The CRN-B network was found to be only very weakly affected by the high-temperature treatment. For CRN-A, in contrast, annealing resulted in significant changes in the topology; the average coordination, for instance, increased from 3.95 to 4.19. Likewise, the energy *increased* from -13.45 eV/atom to -13.39 eV/atom. This clearly indicates that *model CRN-A is not a proper state for GaAs*. Though it would take much longer runs to find out, it is very likely that the system is trying to find a route (through a higher-energy transition state) towards the preferred configuration—one without wrong bonds, i.e., CRN-B. Thus, these high-temperature simulations confirm that CRN-B is indeed a much better model for the structure of *a*-GaAs than CRN-A. In view of this, the structures relaxed at 300 K before annealing will be used for comparing the two models in the discussion that follows.

As noted above, here we used 216-atom unit cells, the largest size we could deal with in our TB simulations, but nevertheless large enough to provide a satisfactory description of amorphous semiconductors.¹⁶ With 64-atom cells, we found ART to lead, in all cases, to the crystalline state, indicating that the configurational space for a system of this size is small enough for ART to find the global minimum. In contrast, for the 216-atom systems, crystallization never occurred—it is very likely much beyond the reach of ART and other simulations—and we therefore conclude that the local minima we find are truly optimized.

IV. STRUCTURAL PROPERTIES

In Fig. 1 are shown ball-and-stick representations of the two *a*-GaAs samples. For CRN-B, wrong bonds are few but one can be seen in the top right quadrant where its presence gives rise to both a five- and a seven-membered ring. It is clear from this figure that the two models, though clearly ordered at short-range—both topologically and chemically—bear no trace of crystallinity. (It is often the case that partly crystalline samples cannot be recognized, because of averaging and thermal agitation, in such quantities as radial distri-

CRN-A



CRN-B

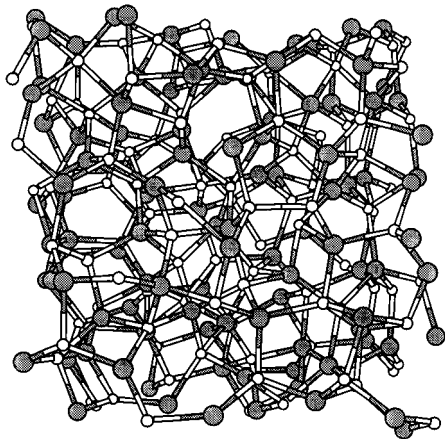


FIG. 1. Ball-and-stick representation of CRN-A and CRN-B after relaxation with a GaAs TB potential; small white circles are As and larger gray circles are Ga atoms.

bution functions and static structure factors.) In fact, based on this visual inspection, it is already evident to a trained eye that the samples are excellent models of the amorphous material.

We now proceed with a more quantitative analysis of the models. First we give, in Table I, some of the usual system-averaged structural quantities—coordination numbers, proportion of wrong bonds, and width of the bond-angle distribution—for our two GaAs models after TB relaxation, both at 0 and at 300 K. Here we do not distinguish between the various types of correlations and treat all atoms on the same footing. The reason for this is that the identity of the atoms prior to the ART relaxation was introduced in an *ad hoc* fashion; since the TB relaxation does not change the connectivity of the network, the two species are still topologically equivalent in the final configuration. This, it turns out, is consistent with previous simulations by Molteni, Colombo, and L. Miglio¹⁷ and by Fois *et al.*¹⁸ which show the two species to behave symmetrically, and is also supported by experiment, which indicates that both As and Ga are fourfold coordinated (taking due account of variations in composition).¹⁹

We first observe that the structural characteristics of both CRN-A and CRN-B satisfy the requirements of a “good” CRN, namely, overall fourfold coordination and small bond-angle deviation. From Table I, it is apparent that CRN-A and CRN-B have a density of coordination defects lower than that of previous models of *a*-GaAs. In particular, both models have a coordination of almost exactly four, i.e., most atoms are perfectly coordinated but a few are undercoordinated (cf. Table I). [In order to define nearest neighbors, we use here the distance corresponding to the minimum following the first maximum of the total radial distribution function (see below), viz., 3.0 Å at 0 K and 3.1 Å at 300 K.] Both networks, therefore, are consistent with experiments.¹⁹ It is also clear from Table I that the finite-temperature models are roughly equivalent to the zero-temperature ones, at least inasmuch as total coordination is concerned. For CRN-B, the total coordination remains constant at 3.95, while for CRN-A, it decreases slightly; the latter may be related to the unstable character of CRN-A for GaAs. Thermal agitation, however, brings about a widening of the distributions of neighbors and bond angles, i.e., the weight is spread over three-, four-, and five-coordinated atoms, leaving essentially unchanged the number of wrong bonds.

The density of wrong bonds in model CRN-A is 14% or

TABLE I. Structural characteristics of the two models for GaAs discussed in the text, at both 0 K and 300 K: distribution of coordination numbers, Z (and nearest-number cutoff distance, r_{NN}), density of wrong bonds, and width of the bond-angle distribution $\Delta\theta$. Also given are the corresponding numbers from other simulations, all at 0 K: SL, Seong-Lewis tight-binding simulations of Ref. 21; MCM, tight-binding simulations of Ref. 17; CP, Car-Parrinello simulations of Ref. 18.

	CRN-A		CRN-B		SL	MCM	CP
	0 K	300 K	0 K	300 K			
$Z=3$	0.046	0.128	0.051	0.118	0.242	0.14	0.219
$Z=4$	0.954	0.845	0.944	0.830	0.598	0.66	0.781
$Z=5$	0	0.026	0.005	0.045	0.129	0.18	0
$Z=6$	0	0.001	0	0.004	0.024		0
$Z=7$	0	0.000	0	0.002	0.007		0
$\langle Z \rangle$	3.95	3.90	3.95	3.95	3.94	4.09	3.83
r_{NN} (Å)	3.0	3.1	3.0	3.1	3.0	3.0	2.8
Wrong bonds (%)	14.1	14.2	3.9	5.2	12.2	12.9	10.0
$\Delta\theta$ (deg)	11.0	14.1	10.8	15.0	17.0	17.0	

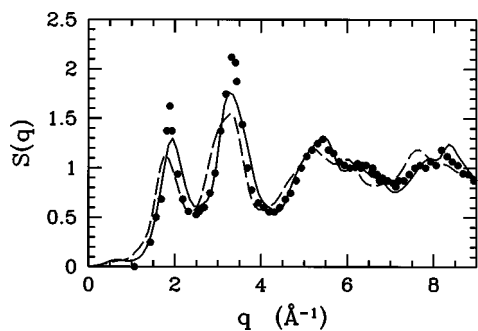


FIG. 2. Total static structure factors for CRN-A (dashed line) and CRN-B (solid line); the dots are the experimental data of Udron *et al.* (Ref. 22).

15%. As discussed earlier, this value was obtained by assigning the identities of atoms on CRN-A such as to minimize the number of wrong bonds, and corresponds quite closely to the “theoretical limit” of 12% for a Polk-type CRN.¹⁵ It is also close to the values obtained in melt-and-quench MD simulations of *a*-GaAs (10–13%, cf. Table I). In contrast, CRN-B, with less than 4% or 5% of wrong bonds, is the closest realization of an “infinite” Connell-Temkin model. Such a low proportion of wrong bonds also seems to be in much better agreement with experiment, which indicates that at most a few percent of wrong bonds are present;²⁰ as will be discussed below, however, the measurements on which this estimate is based turn out to be much less sensitive to the density of wrong bonds than what is usually believed. Finally, visual inspection of Fig. 1 reveals no spatial concentration of wrong bonds; they appear to be homogeneously distributed on both networks.

That CRN-B is a better model for the structure of *a*-GaAs than CRN-A is evident from the configurational energies (cf. Table I, Ref. 4); we also find that the procedure employed here—ART plus TB-MD relaxation—leads, for GaAs, to a better model than the usual melt-and-quench MD approach.

The ability of CRN-B to describe *a*-GaAs can also be assessed from the total static structure factors (SSF’s), at 300 K, presented in Fig. 2: the SSF for CRN-B matches more closely the experimental data²² than that for CRN-A. Unfortunately, the samples used in the experiment suffer from some inhomogeneities; further structural measurements on better-quality material would provide much-needed experimental data for more accurate comparisons.

The partial SSF’s for the two models are shown in Fig. 3. Although they differ in many ways, no evident signature of the presence of wrong bonds in CRN-A can be identified: the differences between the two sets of curves are essentially quantitative, and no peaks appear in one of the partials that are totally absent in the other. However, as we discuss next, the partial radial distribution functions (RDF’s), obtained from the SSF’s by a Fourier transformation, allow a much better interpretation of these differences.

In effect, the partial RDF’s can provide direct, quantitative, evidence of the existence, and proportion, of wrong bonds; they are given in Fig. 4 for our models, from the 300-K runs. The fact that CRN-B is chemically ordered is clearly visible in the partial RDF’s: The unlike-atom partial function, Ga-As, exhibits a strong first-neighbor peak, but very little amplitude at the second and fourth nearest-

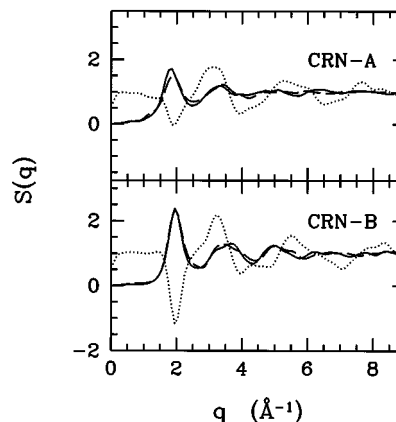


FIG. 3. Partial static structure factors for the two models, as indicated; the dotted, dashed, and solid lines are for the Ga-Ga, Ga-As, and As-As partial correlations.

neighbor distances. In contrast, the like-atom partial RDF’s, Ga-Ga and As-As, have essentially no nearest neighbors, but exhibit strong second and fourth nearest-neighbor peaks. Thus, chemical order “filters out” the shell structure of the material (on the short and intermediate length scales). As a result, the large split peak of the Ga-As correlation function in the range 3.5–7 \AA , which corresponds to third nearest neighbors, can be clearly isolated from others. This is important because this peak corresponds to the various possible dihedral conformations; here we find that the two subpeaks correspond to dihedral angles of 60 and 180 degrees, as we indeed find below through a direct calculation of the dihedral angle distribution.

These results point to the importance of measuring the partial RDF’s (or SSF’s). Because Ga and As are close to one another, however, only the total RDF is available from x-ray or other scattering measurements. This is true also of EXAFS (Ref. 22) for which it is difficult to distinguish the atomic type in the nearest-neighbor shell. This is unfortunate because, as can be seen in Fig. 4, most of the information on wrong bonds is lost in the weighted sum over the partial RDF’s: the total RDF’s for the two models are almost iden-

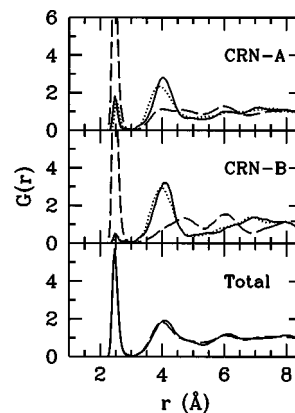


FIG. 4. Partial radial distribution functions for the two models, as indicated; the dotted, dashed, and solid lines are for the Ga-Ga, Ga-As, and As-As partial correlations, respectively. The lower panel gives the total (unweighted) radial distribution function for CRN-A (dashed line) and CRN-B (solid line).

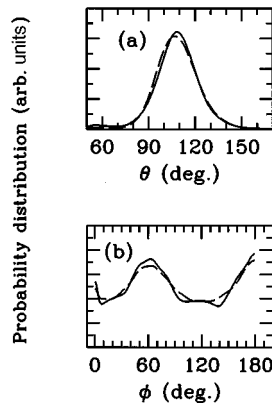


FIG. 5. Distributions of (a) bond and (b) dihedral angles for CRN-A (dashed lines) and CRN-B (full lines).

tical over the whole range of distances of interest, as can be seen in Fig. 4.

The quality of the models can also be inferred from the distributions of bond and dihedral angles. In the case of *a*-Si, the width of the bond-angle distribution at 0 K is found experimentally to lie in the range 10° – 12° ,³ in accord with recent, fully optimized, WWW models.¹⁶ From MD simulations of *a*-Si, and more recently *a*-GaAs, typical values for this quantity are in the range 15° – 17° ; in the case of *a*-GaAs, further, the distribution of bond angles is observed to be asymmetric,^{17,21} biased towards smaller angles, manifest in the presence of a significant number of over-coordinated atoms. These results could be seen as supporting the analysis of Connell and Temkin, who have found their model to have a wider distribution of bond angles than Polk, owing to the additional constraint on the parity of atomic rings. However, we find here that CRN-A and CRN-B both have a bond-angle distribution of width about 11° (at 0 K; cf. Table I), very much in agreement with experiment. Both distributions, moreover, are centered closely on the ideal tetrahedral angle and are almost Gaussian. The similarity between the angular distributions for two such different models reflects the ability of the network to reorganize in spite of topological constraints on the formation of odd-membered rings.²³

We now turn to dihedral angles, i.e., angles between second-nearest-neighbor bonds. Connell and Temkin found, in their model, staggered configurations ($\phi = 60^\circ$) to be four times more numerous than in the Polk model, concluding that this preference for staggered configurations should be a signature of the absence of odd-membered rings, i.e., characteristic of CRN-B-type materials. We find no support for such a conclusion here: as can be seen in Fig. 5(b), our two models exhibit essentially identical dihedral-angle distributions.

As demonstrated in Ref. 4, *a*-GaAs and *a*-Si form networks that are topologically different. Structural signatures of these differences, however, as we have seen here by comparing models CRN-A and CRN-B, are extremely difficult to extract from experiment or even from computer models; it seems to show up clearly, in fact, only in quantities that cannot be measured directly, namely, the number of wrong bonds or ring statistics. Thus, most measurable quantities appear to be unaffected by the constraint on wrong bonds. It

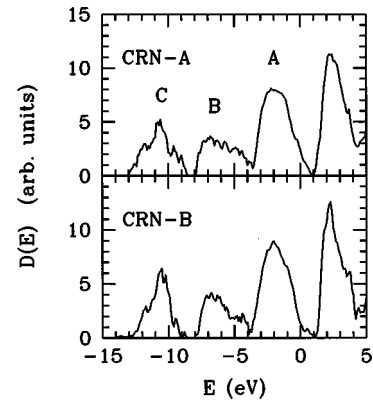


FIG. 6. Electronic densities of states for the two models, as indicated. The identification of the peaks is discussed in the text.

should be noted that even though the experimental precision required to decide between the two models on the basis of their total SSF's (or RDF's) can easily be achieved (cf. Figs. 2 and 4), the interpretation of the small differences is not simple, as they could be due to variations in the modes of preparation, details of the electronic potentials that could affect the structure without changing the connectivity, etc. The problem could, however, be resolved through measurements of the *partial* SSF's, as discussed above; unfortunately, this does not seem to be possible at present.

V. ELECTRONIC PROPERTIES

The electronic densities of states (DOS's) for our two samples, CRN-A and CRN-B, are displayed in Fig. 6. These were obtained by averaging over the MD trajectories for a period of 3.5 ps at 300 K. As discussed in Refs. 24 and 25, the bands in the DOS can be roughly ascribed as follows: the lowest-lying band, labeled *C* in Fig. 6, is As *s*-like while the next one, *B*, arises from Ga *s* and some As *p* states; the gap between this band and the following one is the "ionicity" gap. Just below the forbidden gap, band *A* is composed of As *p* and Ga *p* states. In a crystal, the gap is direct and has a width of 1.55 eV.

X-ray-photoemission-spectroscopy (XPS) measurements of amorphous GaAs have been interpreted as indicating that the material is essentially chemically ordered.²⁰ Probing the valence band from the gap down to about -15 eV, XPS reveals relatively little difference from the crystalline state except for the filling of the minimum between the first (*A*) and second (*B*) peak and a shift of 0.5 eV upwards of the third peak (*C*). However, upon comparing the DOS for our two networks (Fig. 6), one sees an increased contribution in model CRN-A of the high-energy side of the low-lying As *s* band (*C*), almost forming an additional peak; this is due to wrong As-As bonds, as was also shown in Refs. 24 and 25. The width of the gap at 300 K between this band and the following mixed band, -1.5 eV in the crystal, is reduced to about 0.9 eV in CRN-B and 0.5 eV in CRN-A.

Another manifestation of the presence of wrong bonds is visible in the high-energy tail of the *B* band, which is much broader than in the crystal.^{24,25} The added contributions at about -4.5 eV *must* be due to wrong bonds since the structural properties of the two models are very similar except for

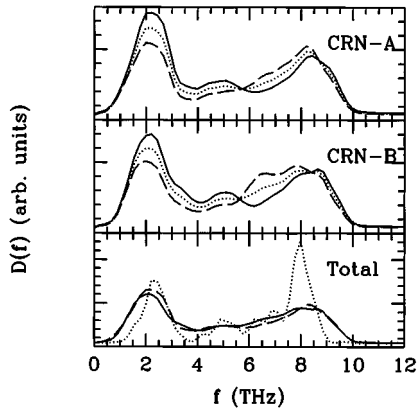


FIG. 7. Partial and total vibrational densities of states for the two models, as indicated. Dashed lines are for Ga atoms, solid lines for As and dotted lines are the totals. The lower panel presents a comparison of CRN-A (dashed line) and CRN-B (solid line) with the crystal (dotted line).

the number of such defects. This is in agreement with the discussion presented in Ref. 21.

It is clear from the comparison between the two models that although present, the effects of the existence of wrong bonds on the electronic structure of the material are much weaker than can hopefully be measured using techniques such as XPS. Thus, the observed similarities in the XPS spectra of *a*- and *c*-GaAs *cannot* be taken as evidence that the amorphous material is chemically ordered,²⁰ though our calculations do show that this is indeed the case.

Disorder influences strongly the gap between valence and conduction bands. The value for this quantity has been reported in the literature to lie in the range 0.61–1.45 eV.²⁶ Although the gap in the CRN-A sample is about 50% smaller than the one for CRN-B, both are substantially smaller than in the crystal. In particular, this value should depend significantly on the method of preparation of amorphous GaAs and is probably not a very good measure of the bond concentration.²⁷

VI. VIBRATIONAL PROPERTIES

We have calculated the vibrational densities of states (VDOS's) of our two models by Fourier transforming the velocity autocorrelation function averaged over 3.5 ps at 300 K; they are displayed in Fig. 7. Experimentally, this quantity can be extracted from Raman spectroscopy measurements since amorphous networks do not have forbidden symmetries so that all vibrational modes are allowed and measured. A multiple-order Raman scattering study of *a*-GaAs has recently been reported.²⁸ The VDOS extracted from these data reveals two broad peaks, at about 2.3 and 8.3 THz, corresponding to the transverse acoustic and optic modes, respectively, with a wide, almost featureless band in between. At variance with the simulation results of Molteni, Colombo, and Miglio,¹⁷ the TO peak is very much present experimentally, with a weight larger than that of the TA peak.

From our results—Fig. 7—we see that the VDOS for our two model networks are very similar: one difference is perhaps a slight shift of weight from the TA to the TO peak for CRN-B compared to CRN-A. The great similarity in the

VDOS of our two models indicates that this quantity, also, is rather insensitive to the presence of wrong bonds; this would not be the case, however, if the two species differed appreciably in mass or elastic properties. In a recent Car-Parrinello simulation of *a*-InP, for instance, a high-energy peak in the partial P-P VDOS has been identified as arising from wrong bonds;²⁹ because In is significantly heavier than P, the corresponding peak for In-In is lost in the “normal” continuum of states.

Although the agreement between simulation and experiment is satisfactory, a discrepancy remains regarding the relative amplitude of the two peaks. The weight of the TA peak is slightly larger than that of the TO peak in our simulation while the opposite is true experimentally. This difference indicates that “real” *a*-GaAs would have even less coordination defects than our model. Indeed, the TA peak is associated with bond-bending modes that are relatively insensitive to the local order as long as the stress is small, while the TO peak, depends critically on the existence of the tetrahedral symmetry around each atom;^{30,31} any coordination defect causes decrease of this peak. This is in fact clearly evident if we compare our results with those of Molteni, Colombo, and Miglio,¹⁷ whose structure contains a much higher density of coordination defects than ours and shows almost no TO peak. Based on this, therefore, and on the agreement of our calculated DOS with experiment, we conclude that real *a*-GaAs must be almost perfectly fourfold coordinated.

VII. CONCLUDING REMARKS

Using a recently proposed event-based Monte Carlo optimization method, the activation-relaxation technique of Barkema and Mousseau,⁸ we have constructed a model of *a*-GaAs with a minimum of wrong bonds corresponding to an “infinite” Connell-Temkin model (CRN-B). This model is found to be energetically favorable over the traditional Polk-type continuous random network (CRN-A). The CRN-B model of *a*-GaAs represents, to the best of our knowledge, the best realization to date of this material, with an almost perfect fourfold coordination, realistic bond-angle distribution, and almost no wrong bonds.

In order to provide insight into the structure of *a*-GaAs, a detailed study of structural, electronic, and vibrational properties of CRN-B has been presented, including a comparison with CRN-A. These results are in agreement with experiment and suggest that “real” *a*-GaAs forms a perfect CRN network, tetravalent and only weakly strained, with a minimum of wrong bonds (ideally none). Our analysis also shows, however, that wrong bonds are extremely difficult to identify experimentally; in particular, indirect measurements (such as XPS and Raman scattering) cannot provide such information. Likewise, diffraction experiments that do not discriminate between the two chemical species are not sufficiently accurate to yield even approximate estimates of the proportion of wrong bonds. Our calculations indicate that only direct measurements of partial radial distribution functions can provide experimental values for the density of wrong bonds. Such measurements, unfortunately, do not seem to be possible at present. The results presented here thus provide a

useful reference for further experimental and theoretical work.

ACKNOWLEDGMENTS

We are grateful to G. T. Barkema for useful discussions. This work was supported by grants from the Natural Sci-

ences and Engineering Research Council (NSERC) of Canada and the "Fond pour la formation de chercheurs et l'aide à la recherche" of the Province of Québec. Part of the calculations were carried out at the "Centre d'applications du calcul parallèle de l'Université de Sherbrooke" (CACPUS). We are grateful to the "Services informatiques de l'Université de Montréal" for generous allocations of computer resources.

-
- *Permanent address: Department of Physics and Astronomy, Ohio University, Athens, OH 45701. Electronic address: mousseau@helios.phy.ohiou.edu
- †Electronic address: lewis@physcn.umontreal.ca
- ¹W. H. Zachariasen, *J. Am. Chem. Soc.* **54**, 3841 (1932).
- ²D. E. Polk, *J. Non-Cryst. Solids* **5**, 365 (1971).
- ³G. A. N. Connell and R. J. Temkin, *Phys. Rev. B* **9**, 5323 (1974).
- ⁴N. Mousseau and L. J. Lewis, *Phys. Rev. Lett.* **78**, 1484 (1997).
- ⁵J. Sarnthein, A. Pasquarello, and R. Car, *Phys. Rev. Lett.* **74**, 4682 (1995).
- ⁶J. C. Phillips, *Bonds and Bands in Semiconductors* (Academic, New York, 1973).
- ⁷F. Wooten, K. Winer, and D. Weaire, *Phys. Rev. Lett.* **54**, 1392 (1985).
- ⁸G. T. Barkema and N. Mousseau, *Phys. Rev. Lett.* **77**, 4358 (1996).
- ⁹F. Wooten and D. Weaire, *Solid State Phys.* **40**, 1 (1987).
- ¹⁰W. H. Press, B. P. Flannery, S. A. Teukolsky, and W. T. Vetterling, *Numerical Recipes* (Cambridge University Press, Cambridge, 1986).
- ¹¹J. Tersoff, *Phys. Rev. B* **39**, 5566 (1989); R. Smith, *Nucl. Instrum. Methods Phys. Res. Sect. B* **67**, 335 (1992); M. Sayed, J. H. Jefferson, A. B. Walker, and A. G. Gullis, *ibid.* **102**, 232 (1995).
- ¹²F. H. Stillinger and T. A. Weber, *Phys. Rev. B* **31**, 5262 (1985).
- ¹³L. Goodwin, A. J. Skinner, and D. G. Pettifor, *Europhys. Lett.* **9**, 701 (1989).
- ¹⁴C. Molteni, L. Colombo, and L. Miglio, *J. Phys. Condens. Matter* **6**, 5243 (1994).
- ¹⁵M.-L. Thèye, A. Gheorghiu, and H. Launois, *J. Phys. C* **13**, 6569 (1980).
- ¹⁶B. R. Djordjević, M. F. Thorpe, and F. Wooten, *Phys. Rev. B* **52**, 5685 (1995).
- ¹⁷C. Molteni, L. Colombo, and L. Miglio, *Phys. Rev. B* **50**, 4371 (1994).
- ¹⁸E. Fois, A. Selloni, G. Pastore, Q.-M. Zhang, and R. Car, *Phys. Rev. B* **45**, 13 378 (1992).
- ¹⁹D. Udron, A.-M. Flank, P. Lagarde, D. Raoux, and M.-L. Thèye, *J. Non-Cryst. Solids* **150**, 361 (1992).
- ²⁰C. Sénémaud, E. Belin, A. Gheorghiu, and M.-L. Thèye, *Solid State Commun.* **55**, 947 (1985).
- ²¹H. Seong and L. J. Lewis, *Phys. Rev. B* **53**, 4408 (1996).
- ²²D. Udron, M.-L. Thèye, D. Raoux, A.-M. Flank, P. Lagarde, and J.-P. Gaspard, *J. Non-Cryst. Solids* **137&138**, 131 (1991).
- ²³Relaxation of models CRN-A and CRN-B with the GSP TB potential for Si yields a width of 9.44° and 9.70°, respectively, indicating that the bond-bending force is a more important factor for determining this quantity.
- ²⁴J. D. Joannopoulos and M. L. Cohen, *Phys. Rev. B* **10**, 1545 (1974).
- ²⁵E. P. O'reilly and J. Robertson, *Phys. Rev. B* **34**, 8684 (1986).
- ²⁶*Semiconductors: Physics of Group-IV Elements and III-V Compounds*, edited by K.-H. Hellwege and O. Madelung, Landolt-Börnstein, New Series, Group III, Vol. 17, Pt. 6.3 (Springer-Verlag, Berlin, 1984), p. 23.
- ²⁷M.-L. Thèye and A. Gheorghiu, *Philos. Mag. B* **52**, 325 (1985).
- ²⁸A. Chehaidar, A. Zwick, R. Carles, and J. Bandet, *Phys. Rev. B* **50**, 5345 (1994).
- ²⁹L. J. Lewis, A. de Vita, and R. Car (unpublished).
- ³⁰N. Mousseau and L. J. Lewis, *Phys. Rev. B* **43**, 9810 (1991).
- ³¹R. Alben, D. Weaire, J. E. Smith, and M. H. Brodsky, *Phys. Rev. B* **11**, 2271 (1975).